Ab initio treatment of final-state spin-orbit interactions:
Photoionization of the 6s electron in cesium

Keh-Ning Huang* and Anthony F. Starace

Behlen Laboratory of Physics, The University of Nebraska, Lincoln, Nebraska 68588
(Received 25 September 1978)

Ab initio theoretical calculations are presented for the cross section, photoelectron angular distribution, and photoelectron spin polarization resulting from photoionization of the 6s electron of cesium. Starting from an initial basis of nonrelativistic Hartree-Fock wave functions, the effect of final-state spin-orbit interaction in the Breit-Pauli approximation is treated exactly. The effect of core relaxation is also examined. Our calculated results agree with recent experimental measurements of the photoionization cross section and the photoelectron spin polarization. Comparison is made with other theoretical calculations. Finally, the length form of the electric dipole interaction operator is shown to be consistent with gauge invariance when one solves for the exact eigenstates of a Hamiltonian containing spin-orbit interactions.

I. INTRODUCTION

The importance of the spin-orbit interaction to the theoretical description of optical transitions in the alkali metals has been known since Fermi's explanation[1] in 1930 of the anomalous doublet line strength ratio for higher members of the principal series of cesium. Fermi used perturbation theory to show that the spin-orbit interaction is repulsive in the $J = \frac{3}{2}$ state and attractive in the $J = \frac{1}{2}$ state, thus leading to differences between the $p_{3/2}$ and $p_{1/2}$ radial wave functions for the excited electron. These differences are sufficient to explain the observed anomalies. More recently, these same differences between the $J = \frac{3}{2}$ and $J = \frac{1}{2}$ radial wave functions of the excited electron have been used to explain and predict a number of interesting effects that may be observed upon photoionization of cesium: The observed[2,3] occurrence of a *nonzero* minimum in the photoionization cross section was explained thusly by Seaton.[4] The occurrence of a large photoelectron spin polarization near the minimum in the photoionization cross section was predicted by Fano[5] and later observed experimentally.[6-9] Finally, the prediction of energy-dependent photoelectron angular distributions was made by Jacobs,[10] by Walker and Waber,[11] and by Marr,[12] but has not yet been verified experimentally.

Despite the intrinsic theoretical interest of the alkali metals generally—in particular of cesium, since it has the largest spin-orbit interaction— all of the theoretical calculations mentioned above and nearly all of the theoretical work on cesium subsequently has been semiempirical.[13-17] The best of the semiempirical calculations are those of Weisheit[15] and of Norcross,[16] who achieve very close agreement with experiment within a few eV of the first ionization threshold. Each of these two calculations incorporates both spin-orbit and polarization potential terms in the semiempirical model potential.

Only three ab initio calculations on cesium are known to us: Chang and Kelly[18] have used Dirac-Fock wave functions to compute the photoionization cross section and the amount of spin polarization; Amusia and Cherepkov[19] have reported random-phase approximation (RPA) calculations for the cesium photoionization cross section in which they account for intershell correlation between the 6s subshell and lower-lying ones; and very recently, Ong and Manson[20] used Dirac-Fock wave functions to calculate the photoelectron angular distribution near threshold. Of these three calculations, the RPA one neglects spin-orbit interactions altogether and gives poor agreement with experiment near the ionization threshold. The Dirac-Fock calculations take into account the spin-orbit interaction of the photoelectron in the field of the screened nucleus, but neglect the spin-other-orbit interaction arising from the Breit interaction.[21] The Dirac-Fock calculations do, however, give qualitative agreement with experiment near the ionization threshold.

In this paper, we present ab initio calculations of the cesium photoionization cross section, photoelectron angular distribution, and photoelectron spin polarization taking proper account of the final-state spin-orbit interaction. That is, in addition to the spin-orbit interaction of the photoelectron in the field of the nucleus, we have evaluated exactly the matrix elements of the mutual spin-orbit operator.[22] This mutual spin-orbit operator arises from the relativistic Breit-Pauli correction[21] to the nonrelativistic Hartree-Fock Hamiltonian. The final-state perturbation matrix elements were then used to obtain improved final-state wave functions in the $J = \frac{3}{2}$ and $J = \frac{1}{2}$ photoelec-

tron channels by means of the K-matrix method.[23,24] In addition, unlike other calculations, ours are carried out using both frozen and relaxed ionic core wave functions in order to demonstrate the effect of core relaxation. In common with all other *ab initio* calculations, we have neglected polarization effects. In common with the Dirac-Fock calculations mentioned above, we have neglected intershell correlations since the $5p$ subshell lies more than 8 eV below the $6s$ subshell.[25] Our results are in qualitative agreement with previous Dirac-Fock calculations, but agree more closely with experiment near threshold than all previous *ab initio* calculations.

In Sec. II we discuss the mutual spin-orbit interaction operator and present our results for its matrix elements. In Sec. III we review briefly the K-matrix method for obtaining improved electric-dipole matrix elements. In Sec. IV we summarize formulas for the photoionization cross section, photoelectron angular distribution, and photoelectron spin polarization. In Sec. V we present our results, compare them with experiment and with other calculations, and discuss our conclusions. Finally, in the Appendix we show that it is the length form of the electric-dipole interaction which is consistent with gauge invariance of a model Hamiltonian containing the spin-orbit interaction.

is a single electron outside closed shells, the mutual spin-orbit interaction may be reduced to an effective one-particle spin-orbit interaction.[22] One may describe the mutual spin-orbit interaction in this case as consisting, firstly, of the direct and exchange contributions to both the spin-self-orbit and the spin-other-orbit interactions of the outer electron in the field of the closed shells, and, secondly, the direct and exchange contributions to both the spin-self-orbit and spin-other-orbit interactions of the closed-shell electrons in the field of the outer electron.[22]

Matrix elements of the spin-orbit operator in Eq. (1) may be evaluated by using graphical methods.[22,28] In this paper we are concerned with photoionization of the $6s$ subshell of cesium in the electric-dipole approximation:

$$Cs\,1s^2\cdots5p^66s\,(^2S_{1/2})$$

$$\xrightarrow[\text{photoionization}]{} Cs^+1s^2\cdots5p^6\epsilon p\,(^2P_{3/2,1/2})\,. \qquad (3)$$

II. SPIN-ORBIT MATRIX ELEMENTS

The quantum electrodynamic interaction between electrons can be approximated, to the lowest order in the fine-structure constant α, by the Breit interaction,[26,27] which in the Pauli approximation gives rise to the mutual spin-orbit interaction (as well as others which are less important).[21] Consequently, the total spin-orbit interaction for many-electron atoms can be written in atomic units as[21]

$$V^{SO} = \tfrac{1}{2}Z\,\alpha^2 \sum_{i=1}^{N} \frac{1}{r_i^3}\,\vec{l}_i\cdot\vec{s}_i + \sum_{i\neq j}^{N} V_{ij}\,, \qquad (1)$$

where the mutual spin-orbit operator is

$$V_{ij} = -\tfrac{1}{2}(\alpha^2/r_{ij}^3)\,(\vec{r}_{ij}\times\vec{p}_i)\cdot(\vec{s}_i+2\vec{s}_j)\,. \qquad (2)$$

In the case of atomic configurations in which there

The spin-orbit matrix elements of interest to us are thus

$$\langle Cs^+1s^2\cdots5p^6\epsilon'p\,(^2P_{1/2})|$$

$$\times V^{SO}|Cs^+1s^2\cdots5p^6\epsilon p\,(^2P_{1/2})\rangle = -\zeta_{\epsilon'p,\,\epsilon p}\,, \qquad (4a)$$

$$\langle Cs^+1s^2\cdots5p^6\epsilon'p\,(^2P_{3/2})|$$

$$\times V^{SO}|Cs^+1s^2\cdots5p^6\epsilon p\,(^2P_{3/2})\rangle = +\tfrac{1}{2}\zeta_{\epsilon'p,\,\epsilon p}\,, \qquad (4b)$$

where

$$\zeta_{\epsilon'p\,\epsilon p} \equiv \tfrac{1}{2} Z\,\alpha^2 \langle 1/r^3 \rangle_{\epsilon'p,\,\epsilon p} + \sum_{n=1}^{5}\ [-4N^0(\epsilon'pns;\epsilon pns) - 4N^{-1}(\epsilon'pns;ns\epsilon p)$$

$$+2N^1(ns\epsilon'p;\epsilon pns) + 2V^0(\epsilon'pns;ns\epsilon p)\,]$$

$$+\sum_{n=2}^{5}\ [-12N^0(\epsilon'pnp;\epsilon pnp) - \tfrac{12}{5}N^0(\epsilon'pnp;np\epsilon p) + \tfrac{42}{5}N^0(np\epsilon'p;\epsilon pnp) - \tfrac{18}{5}N^2(\epsilon'pnp;np\epsilon p)$$

$$+\tfrac{18}{5}N^2(np\epsilon'p;\epsilon pnp) + \tfrac{18}{5}V^1(\epsilon'pnp;np\epsilon p)\,]$$

$$+\sum_{n=3}^{4}\ [-20N^0(\epsilon'pnd;\epsilon pnd) - 2N^{-1}(\epsilon'pnd;nd\epsilon p) - 6N^{-1}(nd\epsilon'p;\epsilon pnd) - \tfrac{6}{7}N^1(\epsilon'pnd;nd\epsilon p)$$

$$+\tfrac{124}{7}N^1(nd\epsilon'p;\epsilon pnd) - \tfrac{72}{7}N^3(\epsilon'pnd;nd\epsilon p) + \tfrac{36}{7}N^3(nd\epsilon'p;\epsilon pnd)$$

$$-2V^0(\epsilon'pnd;nd\epsilon p) + \tfrac{36}{7}V^2(\epsilon'pnd;nd\epsilon p)\,]\,. \tag{5}$$

In Eq. (5) the radial integrals are defined as follows:

$$\left\langle \frac{1}{r^3} \right\rangle_{\epsilon'p,\,\epsilon p} = \int_0^\infty r^2 dr\, R_{\epsilon'p}(r)\,\frac{1}{r^3}\,R_{\epsilon p}(r); \tag{6}$$

$$N^k(ab;cd) = \frac{\alpha^2}{4}\int_0^\infty r_1^2\,dr_1 \int_0^\infty r_2^2 dr_2 R_a(r_1)R_b(r_2)\,\frac{r_2^k}{r_1^{k+3}}\,\theta(r_1 - r_2)R_c(r_1)R_d(r_2); \tag{7}$$

$$V^k(ab;cd) = \frac{\alpha^2}{4}\int_0^\infty r_1^2\,dr_1 \int_0^\infty r_2^2\,dr_2 R_a(r_1)R_b(r_2)\,\frac{r_<^k}{r_>^{k+3}}\left(r_2\frac{d}{dr_1} - r_1\frac{d}{dr_2}\right)R_c(r_1)R_d(r_2)\,. \tag{8}$$

In the above equations, $R_a(r_1)$ is the radial wave function for the electron state a, and the θ function is defined by

$$\theta(r_1 - r_2) = \begin{cases} 1 & \text{for } r_1 > r_2 \\ 0 & \text{for } r_1 < r_2 \end{cases}. \tag{9}$$

For the diagonal matrix elements we were able to verify that our result in Eq. (5) agrees with that of previous calculations.[22, 29] As a practical consideration, we note that in Eq. (5) the direct N^0 integrals are generally much larger than the other N^l and V^l integrals.

III. K-MATRIX CALCULATION OF IMPROVED DIPOLE MATRIX ELEMENTS

Our zero-order Hamiltonian is the V^{N-1} Hartree-Fock (HF) Hamiltonian[30] in which the occupied ionic orbitals are taken to be either the HF orbitals of the neutral atom (i.e., the frozen-ionic-core approximation) or the HF orbitals of the ion

(i.e., the relaxed-ionic-core approximation). This Hamiltonian is used to generate the continuum p orbitals for the photoelectron. Since in our zero-order approximation the $J = \tfrac{3}{2}$ and $J = \tfrac{1}{2}$ states for the photoelectron are degenerate, we denote a member of the zero-order set of final-state Slater determinants simply by the energy index of the photoelectron:

$$|\epsilon\rangle \equiv |Cs^+ 1s^2 \cdots 5p^6 \epsilon p\,(^2P)\rangle\,. \tag{10}$$

The perturbation Hamiltonian is the spin-orbit operator, given by Eq. (1), which splits the degeneracy between the $J = \tfrac{3}{2}$ and $J = \tfrac{1}{2}$ states in Eq. (10). Matrix elements of the spin-orbit operator between states of the form (10) are given by Eq. (4).

Our aim is to calculate the exact energy eigenstates of the Hamiltonian given by

$$H = H_{HF} + V_J^{so} \tag{11}$$

within the subspace of states of the form (10). In Eq. (11) the subscript J on the spin-orbit operator

indicates explicitly that the spin-orbit interaction is J dependent. The energy eigenstates of Eq. (11) may be written in terms of the reaction matrix $K_J(E)$ of scattering theory as follows[23,24]:

$$|\psi_{JE}^-\rangle = \left(|E\rangle + \mathcal{P} \int d\epsilon \; \frac{|\epsilon\rangle\langle\epsilon|K_J(E)|E\rangle}{E-\epsilon}\right)$$

$$\times \cos\eta_J \exp(-i\eta_J - i\delta) . \qquad (12)$$

In Eq. (12) the symbol $\mathcal{P}$ indicates that the Cauchy principal part is to be taken when integrating over the singularity in the denominator and the integration over the photoelectron energy ϵ implies also a summation over discrete states. The reaction matrix is obtained as the solution of the following integral equation:

$$\langle\epsilon|K_J(E)|E\rangle = \langle\epsilon| V_J^{so}|E\rangle$$

$$+ \mathcal{P} \int d\epsilon' \; \frac{\langle\epsilon|V_J^{so}|\epsilon'\rangle\langle\epsilon'|K_J(E)|E\rangle}{E-\epsilon'} . \qquad (13)$$

The phase shift η_J in the normalization factor $\cos\eta_J$ is defined in terms of the on-the-energy shell reaction matrix as follows:

$$\tan\eta_J = -\pi\langle E|K_J(E)|E\rangle . \qquad (14)$$

Lastly, in Eq. (12) the factor $\exp(-i\eta_J - i\delta)$ (where δ is the HF phase shift of the photoelectron with respect to Coulomb waves[31]) is needed to convert the standing-wave normalization to the incoming-wave normalization as required for photoionization processes.[32,33]

One may obtain an equation for the improved *radial* dipole matrix elements by operating on both sides of Eq. (12) with the operator $\langle 0|\sum_i \vec{r}_i$, where $\sum_i \vec{r}_i$ is the length form of the electric-dipole operator and where $\langle 0|$ denotes the ground state,

$$\langle 0| \equiv \langle Cs\, 1s^2 \cdots 5p^6 6s(^2S)| . \qquad (15)$$

After dropping common angular factors from both sides of the resulting equation, one gets

$$M_{JE} = \left(m_E + \mathcal{P} \int \frac{d\epsilon\, m_\epsilon \langle\epsilon| K_J(E)|E\rangle}{E-\epsilon}\right)$$

$$\times \cos\eta_J \exp(-i\eta_J - i\delta) , \qquad (16)$$

where the zero-order HF radial dipole-length matrix elements are defined by

$$m_\epsilon \equiv \int_0^\infty r^2\, dr\, R_{6s}(r) R_{\epsilon p}(r) . \qquad (17)$$

Alternatively one may operate on both sides of

Eq. (12) with $\langle 0|\sum_i \vec{\nabla}_i$ to obtain an equation identical in form to Eq. (16) for the improved radial dipole-velocity matrix element, $\overline{M}_{JE}$, in terms of the zero-order HF radial dipole-velocity matrix elements,

$$\overline{m}_E \equiv \int_0^\infty r^2\, dr\, R_{6s}(r) \frac{d}{dr} R_{\epsilon p}(r) . \qquad (18)$$

The procedure, then, for obtaining improved radial dipole matrix elements is as follows. First one solves the integral equation (12) by reduction to a set of linear algebraic equations,[24] using matrix elements of V_J^{so} calculated as in Sec. II. Then one calculates the zero-order HF radial dipole matrix elements according to either the length form in Eq. (17) or the velocity form in Eq. (18). Improved radial dipole matrix elements, normalized according to the incoming-wave boundary condition, are obtained then by transforming the zero-order dipole matrix elements according to Eq. (16).

IV. FORMULAS FOR EXPERIMENTALLY MEASURABLE QUANTITIES

All experimentally measurable quantities related to photoionization of cesium near its first ionization threshold may be expressed theoretically in terms of the improved radial dipole matrix elements M_{JE} defined by Eq. (16). Formulas for the photoionization cross section, photoelectron angular distribution, and photoelectron spin polarization are discussed in turn below.

A. Photoionization cross section

The cross section for the photoionization process (3) is given by

$$\sigma(\omega) = (4\pi^2/3c)\omega| m_E|^2 \qquad (19)$$

in the zero-order HF approximation, and by

$$\sigma(\omega) = (4\pi^2/3c)\omega(\tfrac{2}{3}|M_{3/2E}|^2 + \tfrac{1}{3}|M_{1/2E}|^2) \qquad (20)$$

in the improved calculation including final-state spin-orbit interaction. In Eqs. (19) and (20) ω is the photon energy in atomic units (1 a.u. = 27.2108 eV) and $4\pi^2/3c = 2.68909 \times 10^{-18}$ cm^2. The photoelectron energy E is fixed by the photon energy ω according to

$$\omega = E + I_T,$$

where I_T is the theoretical HF binding energy for the 6s electron (in the frozen-core approximation $I_T = 0.123\,668$ a.u., and in the relaxed-core approximation $I_T = 0.123\,348$ a.u.). The form of Eqs. (19) and (20) is based on our normalization[31] of HF

continuum wave functions: we have required the radial wave function for a photoelectron having kinetic energy ϵ (a.u.) to have an asymptotic amplitude $[2/\pi(2\epsilon)^{1/2}]^{1/2}$. Note that if the velocity form for the matrix elements is used, then ω in Eqs. (19) and (20) is replaced by ω^{-1} and the matrix elements M_{JE} are replaced by $\bar{M}_{JE}$. All other theoretical formulas presented below have the same form in both the dipole-length and dipole-velocity approximations.

B. Photoelectron angular distribution

For linearly polarized light incident on an unpolarized target the photoelectron differential cross section (in the electric-dipole approximation) may be written

$$\frac{d\sigma}{d\Omega} = \frac{\sigma}{4\pi}\left[1 + \beta P_2(\cos\theta)\right]. \tag{21}$$

Here σ is the total photoionization cross section, θ is measured with respect to the axis of linear polarization, and β is the asymmetry parameter, which characterizes the energy dependence of the angular distribution. (For unpolarized or circularly polarized incident light β is replaced by

$-\beta/2$ and θ is measured from the direction of the incident light.)

The asymmetry parameter β is determined by the improved radial dipole matrix elements[10]:

$$\beta(E) = \frac{2|M_{3/2E}|^2 + 2(M_{1/2E}M^*_{3/2E} + M^*_{1/2E}M_{3/2E})}{|M_{1/2E}|^2 + 2|M_{3/2E}|^2} \tag{22a}$$

or equivalently

$$\beta(E) = \frac{2|M_{3/2E}|^2 + 4|M_{3/2E}||M_{1/2E}|\cos(\eta_{3/2} - \eta_{1/2})}{|M_{1/2E}|^2 + 2|M_{3/2E}|^2}. \tag{22b}$$

Note that in the absence of spin-orbit interaction the two dipole amplitudes become equal and β assumes the energy-independent value of 2. In the presence of spin-orbit interaction, $\beta = +1$ when $|M_{1/2E}| = 0$ and $\beta = 0$ when $|M_{3/2E}| = 0$.

C. Photoelectron spin polarization

The spin polarization of photoelectrons ejected by circularly polarized light incident on unpolarized cesium atoms has been shown by Fano[5] to be given by:

$$P(E) = \frac{|M_{3/2E}|^2 + \frac{2}{9}|M_{3/2E} - M_{1/2E}|^2 - \frac{1}{9}|M_{3/2E} + 2M_{1/2E}|^2}{|M_{3/2E}|^2 + \frac{2}{9}|M_{3/2E} - M_{1/2E}|^2 + \frac{1}{9}|M_{3/2E} + 2M_{1/2E}|^2} \tag{23a}$$

or equivalently,

$$P(E) = \frac{5|M_{3/2E}|^2 - |M_{1/2E}|^2 - 4|M_{3/2E}||M_{1/2E}|\cos(\eta_{3/2} - \eta_{1/2})}{6|M_{3/2E}|^2 + 3|M_{1/2E}|^2} \tag{23b}$$

One sees that in the absence of spin-orbit interaction the equality between $M_{3/2E}$ and $M_{1/2E}$ gives $P = 0$. In the presence of spin-orbit interaction, one sees that $P = \frac{5}{6}$ when $M_{1/2E} = 0$ and $P = -\frac{1}{3}$ when $M_{3/2E} = 0$.

D. Fano parameter X

In the limit that the phase shift difference $\eta_{3/2} - \eta_{1/2}$ is very small, one may approximate $\cos(\eta_{3/2} - \eta_{1/2})$ by unity. In this case both the angular distribution asymmetry parameter $\beta(E)$ and the spin-polarization parameter $P(E)$ may be expressed in terms of the Fano parameter $X(E)$ (Ref. 5):

$$X(E) \equiv (2|M_{3/2E}| + |M_{1/2E}|)/(|M_{3/2E}| - |M_{1/2E}|). \tag{24}$$

Thus the asymmetry parameter in Eq. (22) may be written as[12]

$$\beta(E) = 2[X(E)^2 - 1]/[X(E)^2 + 2] \tag{25}$$

and the polarization parameter in Eq. (23) may be written[5]

$$P(E) = [2X(E) + 1]/[X(E)^2 + 2]. \tag{26}$$

A similar formula for the photoelectron spin-polarization resulting from unpolarized light incident

TABLE I. Photoionization data for Cs $6s_{1/2} \rightarrow \epsilon p_{3/2,1/2}$ using frozen ion core.

Photoelectron energy ϵ		Photoionization cross section [a,b] σ (Mb)	Asymmetry parameter [b] β	Polarization parameter [b] P	Fano parameter [b] X
(a.u.)	(eV)				
0.000	0.000	0.1546 (0.0386)	+1.592 (+0.437)	+0.552 (+0.967)	+3.572 (+1.355)
0.020	0.544	0.0212 (0.0204)	−0.472 (−0.302)	+0.948 (−0.214)	+0.651 (−0.778)
0.030	0.816	0.0147 (0.0275)	−0.994 (+0.532)	+0.458 (−0.462)	−0.040 (−1.446)
0.070	1.905	0.0171 (0.0566)	+0.306 (+1.527)	−0.419 (−0.434)	−1.242 (−3.285)
0.090	2.449	0.0199 (0.0672)	+0.639 (+1.629)	−0.477 (−0.401)	−1.554 (−3.790)
0.120	3.265	0.0254 (0.0760)	+1.119 (+1.735)	−0.496 (−0.353)	−2.220 (−4.587)
0.160	4.354	0.0295 (0.0749)	+1.351 (+1.775)	−0.472 (−0.330)	−2.703 (−5.025)

[a] Calculated using theoretical binding energy of 3.3651 eV; experimental binding energy is 3.8938 eV.

[b] Results given using dipole-length (dipole-velocity) formula.

on polarized cesium atoms has been given by Baum et al.[7,9]

V. RESULTS AND DISCUSSION

Our results for the photoionization cross section, photoelectron angular distribution, photoelectron spin polarization, and Fano parameter X associated with $6s$ photoionization are presented in Figs. 1–6 together with the results of experiment and other theoretical calculations. For the convenience of other researchers, we also present our frozen-core and relaxed-core results numerically at a few energies in Tables I and II, respectively. Before we discuss each of our results in detail, three general comments are in order. Firstly, our calculations indicate that the factor $\cos(\eta_{3/2} - \eta_{1/2})$ in Eqs. (22b) and (23b) varies only between 0.996 and 0.998 within the first few eV of the ionization threshold. Hence, we have found that Eqs. (25) and (26) are very good approximations for $\beta(E)$ and $P(E)$, respectively, although all our results use the exact expressions in Eqs.

(22b) and (23b). Secondly, as shown in the Appendix, which is an extension of previous work,[34] only the dipole-length matrix elements are consistent with gauge invariance of the Hamiltonian in Eq. (11) and in that sense are to be preferred. However, we have also calculated the dipole-velocity matrix elements since the Dirac-Fock calculations use the relativistic form of the dipole-velocity approximation. Interestingly, our dipole-length results are the ones that agree most closely with the Dirac-Fock dipole-velocity results. Lastly, since the semi empirical calculations of Weisheit[15] and Norcross[16] agree very well with recent experimental results, we only compare our results to the semiempirical calculations at energies for which there are no experimental results.

A. Photoionization cross section

Our theoretical results for the $6s$ photoionization cross section are presented in Figs. 1 and 2. In Fig. 1 we demonstrate the effect of spin-orbit interactions by comparing the zero-order HF cal-

TABLE II. Photoionization data for Cs $6s_{1/2} \rightarrow \epsilon p_{3/2,1/2}$ using relaxed ion core.

Photoelectron energy ϵ		Photoionization cross section [a,b] σ (Mb)	Asymmetry parameter [b] β	Polarization parameter [b] P	Fano parameter [b] X
(a.u.)	(eV)				
0.000	0.000	0.1124 (0.0253)	+1.552 (+0.112)	+0.578 (+0.997)	+3.382 (+1.084)
0.025	0.680	0.0231 (0.0208)	+0.325 (+0.315)	+0.981 (−0.421)	+1.257 (−1.250)
0.035	0.952	0.0137 (0.0302)	−0.538 (+0.946)	+0.932 (−0.499)	+0.601 (−1.924)
0.070	1.905	0.0151 (0.0567)	+0.294 (+1.604)	−0.416 (−0.410)	−1.232 (−3.644)
0.120	3.265	0.0274 (0.0716)	+1.316 (+1.773)	−0.478 (−0.333)	−2.610 (−4.985)

[a] Calculated using theoretical binding energy of 3.3564 eV; experimental binding energy is 3.8938 eV.

[b] Results given using dipole-length (dipole-velocity) formula.
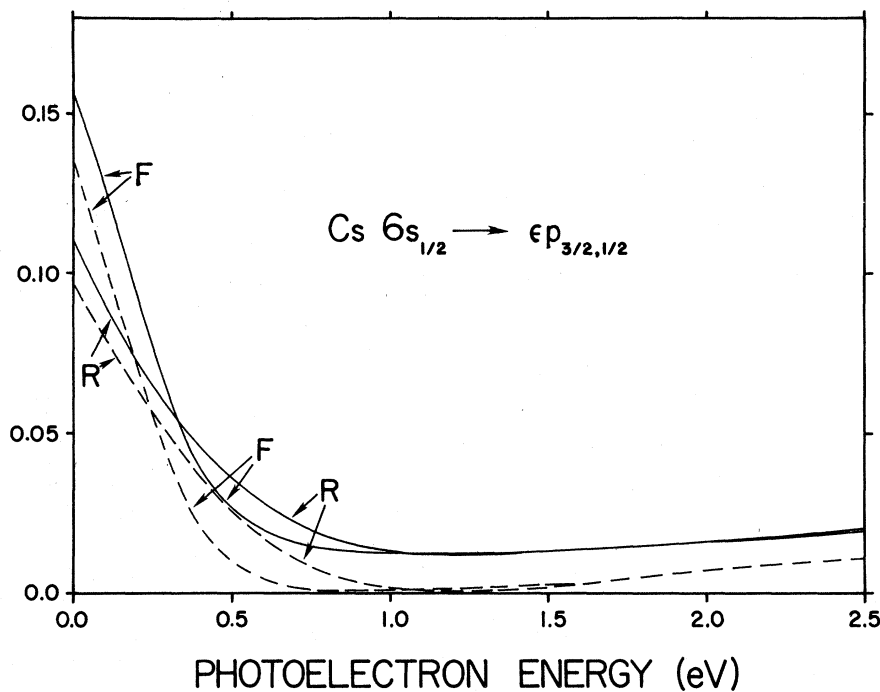
FIG. 1. Cross section for photoionization of the 6s electron in cesium vs photoelectron energy (eV): ---, HF results; —, results including effect of spin-orbit interactions. Results are presented in both the frozen-core approximation (F) and the relaxed-core approximation (R). For clarity, only dipole-length results are shown.
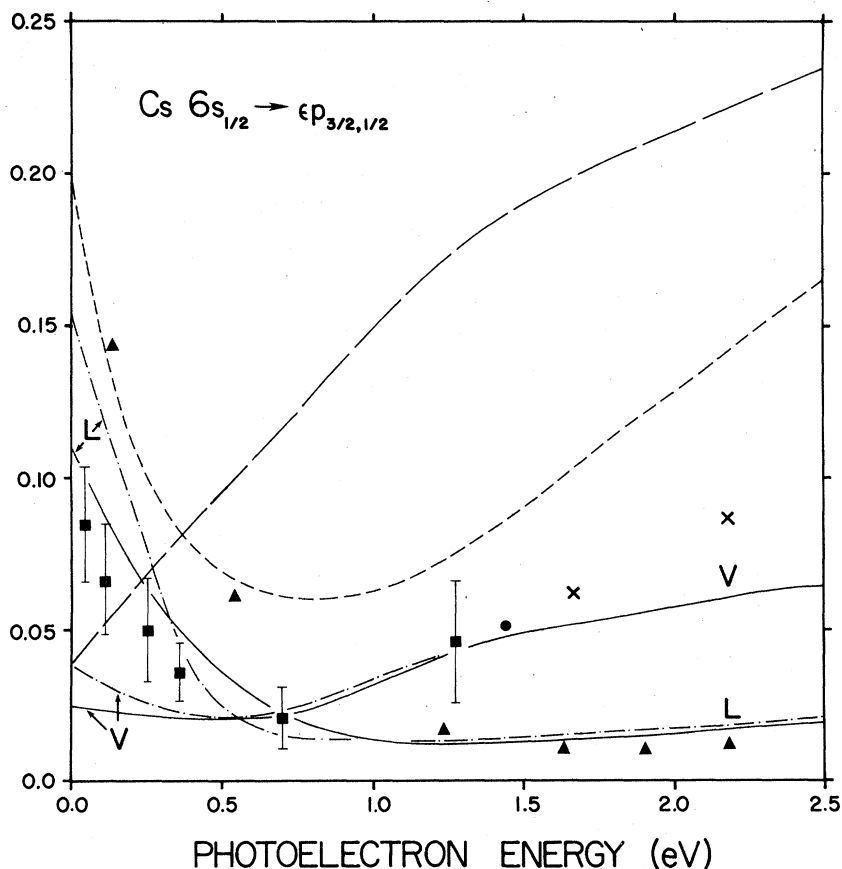
FIG. 2. Cross section for photoionization of the 6s electron in cesium vs photoelectron energy (eV): —, present relaxed-core results in dipole-length (L) and dipole-velocity (V) approximation; −•−, present frozen-core results in dipole-length (L) and dipole-velocity (V) approximation; ---, experimental results of Marr and Creek (Ref. 36); ■, experimental results of Cook et al. (Ref. 35); ●, semiempirical calculations of Norcross (Ref. 16); ×, semiempirical calculation of Weisheit (Ref. 15); ▲, Dirac-Fock calculation of Chang and Kelly (Ref. 18); long dashed line, RPA calculation of Amusia and Cherepkov (Ref. 19).

culations with the calculations including spin-or-
bit interactions. The calculations have been car-
ried out in both the frozen-core and relaxed-core
approximations. The major effect of final-state
spin-orbit interactions is to remove the zero min-
imum appearing in the HF calculations. This ef-
fect is caused by different spin-orbit shifts of the
cross-section minima in the $J = \frac{3}{2}$ and $J = \frac{1}{2}$ photo-
electron channels [cf. Eq. (20)].

Our calculations including spin-orbit interac-
tion are compared with experiment in Fig. 2. For
photoelectron energies in the range $0 \leq \epsilon \leq 0.7$ eV,
our dipole-length relaxed-core results are in ex-
cellent agreement with the recent experimental
measurements of Cook et al,[35] who used a laser to
ionize an atomic beam of cesium atoms and detect-
ed the resulting ions. In this energy region, our
relaxed-core results agree also with the relative
cross-section measurement of Mohler and Boeck-
ner,[2] who photoionized a low-pressure gas of ces-
ium atoms and detected the ions photoelectrically.
We have not plotted the results of Mohler and
Boeckner,[2] however, since if we normalize them
to our relaxed-core result at threshold they fall
within the error bars of Cook et al.[35] We agree
only qualitatively in this energy region with the
photographic absorption measurements of Marr and
Creek,[36] whose results are higher than ours by a
factor of about 2. For photoelectron energies in
the range $0.7 \leq \epsilon \leq 2.5$ eV our dipole-length results
do not rise significantly, as do the experimental
results, although curiously our velocity results do
show such a rise.

In comparison with other theoretical results,

Fig. 2 shows that our dipole-length calculations
agree qualitatively with the Dirac-Fock calcula-
tions of Chang and Kelly.[18] Our results, however,
are closer to the recent experimental measure-
ments[35] than the Dirac-Fock results in the energy
range $0 \leq \epsilon \leq 0.7$ eV, after which our results con-
verge on the Dirac-Fock results. The RPA results
of Amusia and Cherepkov[19] are qualitatively differ-
ent from both our dipole-length results and from
experiment since they rise above threshold rather
than fall. It should be noted that the RPA calcula-
tions do not include spin-orbit interactions, but
do include intershell correlations. However,
since a minimum in the photoionization cross sec-
tion occurs in the zero-order HF calculations,
as shown in Fig. 1, the neglect of spin-orbit inter-
actions in the RPA calculation is certainly not the
reason for the absence of a minimum in the RPA
cross section. At higher energies the rising RPA
cross section is qualitatively similar to, but much
larger than, both the experimental results[35,36]
and the semiempirical calculations.[15,16]

B. Angular distribution asymmetry parameter

Our relaxed-core and frozen-core results for
the photoelectron angular distribution asymmetry
parameter are shown in Figs. 3 and 4, respect-
ively. Our results are obtained using the exact
formula in Eq. (22). However, our calculations
indicate that the phase shift difference $\eta_{3/2} - \eta_{1/2}$
is very small: it starts at -0.075 rad at threshold
and rises to -0.086 rad at 0.4 a.u. kinetic energy.
Thus the angular distribution asymmetry parame-
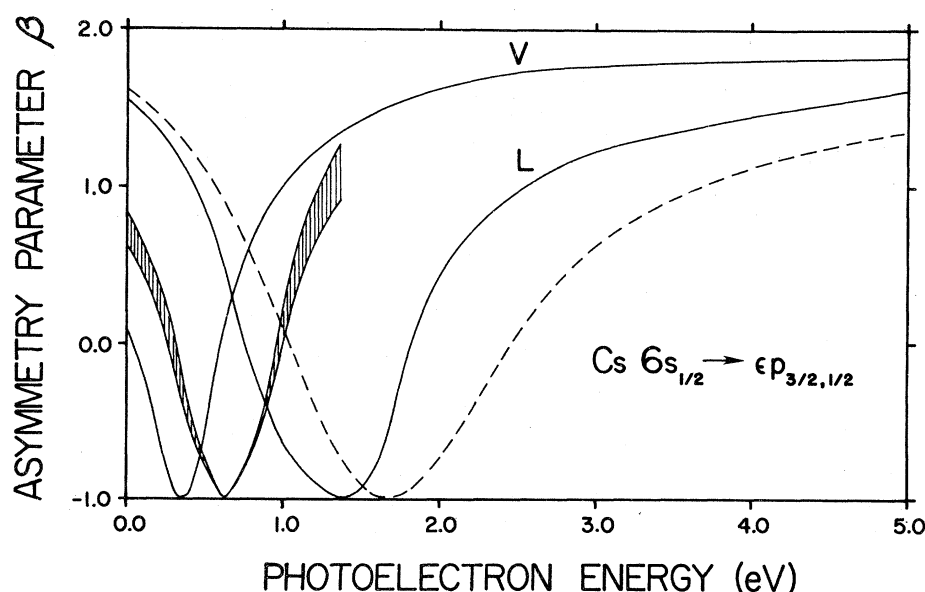
FIG. 3. Angular distri-
bution asymmetry param-
eter $\beta(E)$ vs photoelectron
energy (eV): —, present
relaxed-core results in
dipole-length (L) and di-
pole-velocity (V) approxi-
mation; shaded band, in-
ferred experimental re-
sults obtained from data of
Baum et al. (Ref. 9) for
$X(E)$; ---, Dirac-Fock cal-
culation of Ong and Man-
son (Ref. 20).
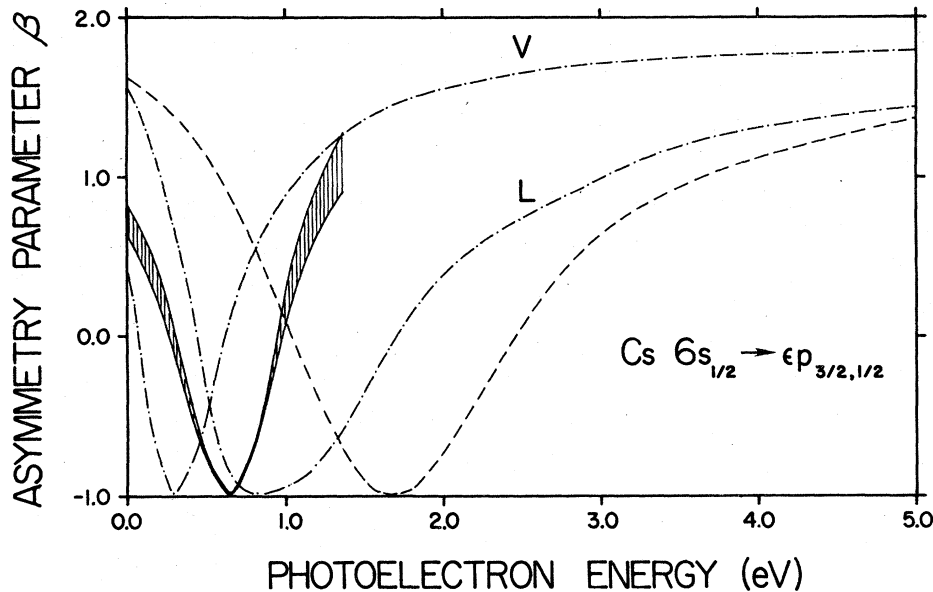
FIG. 4. Angular distribution asymmetry parameter $\beta(E)$ vs photoelectron energy (eV); $-\cdot-$, present frozen-core results in dipole-length (L) and dipole-velocity (V) approximation; shaded band, inferred experimental results obtained from data of Baum *et al.* (Ref. 9) for $X(E)$; $---$, Dirac-Fock calculation of Ong and Manson (Ref. 20).

ter $\beta(E)$ is to a very good approximation determined by the Fano parameter $X(E)$ defined by Eq. (24). Since there are no direct experimental measurements of $\beta(E)$, in Figs. 3 and 4 we have plotted an inferred experimental result obtained by substituting in Eq. (25) the experimentally derived values for $X(E)$ of Baum *et al.*[9] Figures 3 and 4 show that our dipole-length and dipole-velocity results lie on either side of the inferred experimental results. Furthermore, the figures show that our relaxed-core dipole-length results are the ones in closest agreement with the Dirac-Fock

dipole-velocity results of Ong and Manson.[20] We note also that the Dirac-Fock calculations of Ong and Manson[20] are consistent with those of Chang and Kelly[18]: if Chang and Kelly's results for $X(E)$ are substituted in Eq. (25) they give results for $\beta(E)$ that are nearly the same as the results of Ong and Manson using Eq. (22).

C. Photoelectron spin-polarization parameter

The spin polarization of photoelectrons resulting from ionization of unpolarized cesium atoms by
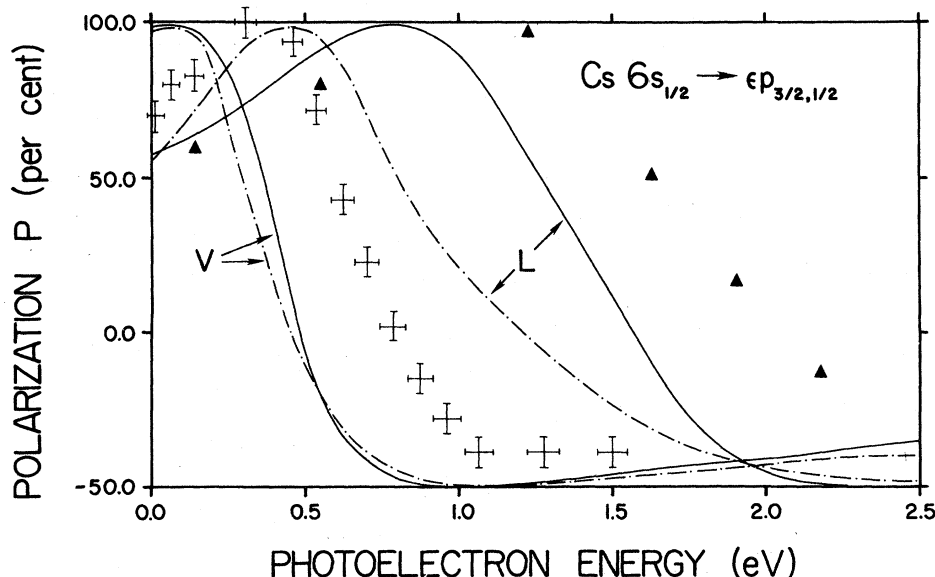
FIG. 5. Photoelectron spin polarization parameter $P(E)$ vs photoelectron energy (eV): $-$, present relaxed-core results in dipole-length (L) and dipole-velocity (V) approximation; $-\cdot-$, present frozen-core results in dipole-length (L) and dipole-velocity (V) approximation; crosses, experimental results of Heinzmann *et al.* (Ref. 8); ▲ Dirac-Fock calculation of Chang and Kelly (Ref. 18).

circularly polarized light has been measured directly by Heizmann *et al.*[8] whose results are shown in Fig. 5. Also shown are our relaxed-core and frozen-core results obtained using the exact Eq. (23). Results obtained using the approximate Eq. (26) are within 1% of those obtained using the exact Eq. (23) due to the smallness of the phase shift difference, as noted above. The figure shows that the dipole-length and dipole-velocity results bound the experimental results and that the frozen-core dipole-length results are closer to experiment than the relaxed-core dipole-length results. Also, our relaxed-core dipole-length results are the ones that agree best with the Dirac-Fock dipole-velocity results of Chang and Kelly.[18]

D. Fano parameter X

Due to the smallness of the phase shift difference $\eta_{3/2} - \eta_{1/2}$, the information contained in our calculated results for $\beta(E)$ and $P(E)$ may be conveniently summarized by the Fano parameter $X(E)$ defined by Eq. (24). Figure 6 presents our results for the parameter $X(E)$ in both the frozen-core and the relaxed-core approximations. As expected from our calculations for $\beta(E)$ and $P(E)$, the dipole-length and dipole-velocity results bound both the experimentally derived values for $X(E)$ of Baum *et al.*[9] and the semiempirical results of Weisheit[15] and Norcross.[16] Whereas our relaxed-core results for the photoionization cross

section agree best with experiment, in the case of the parameter $X(E)$ our frozen-core calculations are closer to experiment that the relaxed-core calculations in the energy region within 2 eV above threshold. As in the calculations of σ, β, and P, our relaxed-core dipole-length results for $X(E)$ are the ones that are closest to the Dirac-Fock dipole-velocity results of Chang and Kelly.[18]

E. Conclusions

In our *ab initio* calculations we have examined the effects of core relaxation and spin-orbit interaction on experimentally measurable quantities associated with 6s photoionization in cesium. The final-state spin-orbit interactions have been treated in the Breit-Pauli approximation as a perturbation on the nonrelativistic HF Hamiltonian. Our results are in better agreement with experiment near the ionization threshold than relativistic Dirac-Fock calculations that ignore the Breit correction to the single-particle Hamiltonian. The effect of core relaxation is threefold: it reduces the 6s electron binding energy, it shifts the zero in the HF radial dipole matrix elements, and it reduces the magnitude of the spin-orbit matrix elements. A merit of the present approach is the disentangling of various effects on experimentally measurable quantities. Intershell correlation effects can easily be incorporated in our approach, and are presently under investigation.[37]
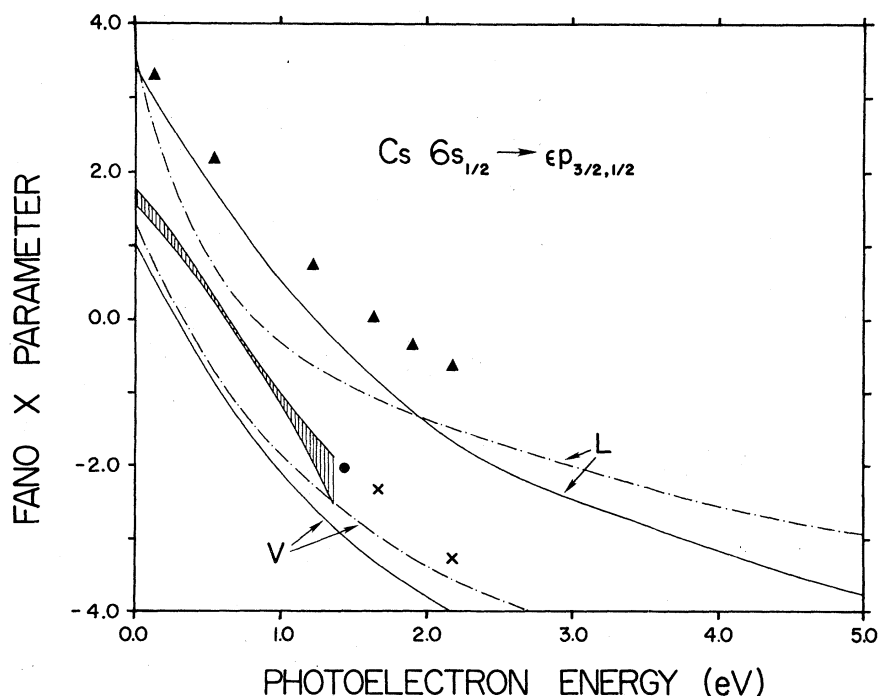
FIG. 6. Fano parameter $X(E)$ vs photoelectron energy (eV); —, present relaxed-core results in dipole-length (L) and dipole-velocity (V) approximation; —·—, present frozen-core results in dipole-length (L) and dipole-velocity (V) approximation; shaded band, experimental results of Baum *et al.* (Ref. 9); ●, semiempirical calculation of Norcross (Ref. 16); ×, semiempirical calculation of Weisheit (Ref. 15); ▲, Dirac-Fock calculation of Chang and Kelly (Ref. 18).

APPENDIX

We demonstrate here that the length form of the electric-dipole interaction operator is the one which is consistent with gauge invariance of the Schrödinger equation corresponding to a Hamiltonian containing the spin-orbit interaction in Eq. (1). We consider explicitly the model Hamiltonian in Eq. (11). Gauge invariance requires that in the presence of electromagnetic radiation the momentum operators in Eq. (11), including those in the spin-orbit interaction, are replaced by

$$\vec{p}_i \rightarrow \vec{p}_i + \vec{A}(\vec{r}_i)/c. \tag{A1}$$

[Note that for this purpose l_i in Eq. (1) should be written as $\vec{r}_i \times \vec{p}_i$.] In the electric-dipole approximation, the electromagnetic field is constant over atomic distances, so that $\vec{A}(\vec{r}_i) = \vec{A}$. To first order in $\vec{A}/c$ the interaction operator describing the coupling with the electromagnetic radiation field is thus

$$H_{\text{int}} = H_{\text{int}}^{\text{HF}} + H_{\text{int}}^{\text{so}} \;, \tag{A2}$$

where

$$H_{\text{int}}^{\text{HF}} = \frac{i}{\hbar}\left[H_{\text{HF}}, \; \sum_{i=1}^{N} \vec{r}_i \right] \cdot \frac{\vec{A}}{c} \tag{A3}$$

and

$$H_{\text{int}}^{\text{so}} = \frac{1}{2} Z \alpha^2 \sum_{i=1}^{N} \frac{1}{r_i^{3}} \, (\vec{s}_i + \vec{r}_i) \cdot \frac{\vec{A}}{c}$$

$$- \frac{1}{2}\alpha^2 \sum_{i \neq j}^{N} \frac{1}{r_{ij}^{3}} [(\vec{s}_i + 2\vec{s}_j) \times \vec{r}_{ij}] \cdot \frac{\vec{A}}{c} \;. \tag{A4}$$

Equation (A3), which gives the interaction operator for the coupling of electrons described by a HF Hamiltonian with the electromagnetic field, has been derived in Ref. 34. A simple calculation shows that Eq. (A4) may be written in the alternative form,

$$H_{\text{int}}^{\text{so}} = \frac{i}{\hbar}\left[V^{\text{so}}, \; \sum_{i=1}^{N} \vec{r}_i \right] \cdot \frac{\vec{A}}{c} \;, \tag{A5}$$

where V^{so} is defined by Eqs. (1) and (2). Combining Eqs. (A3) and (A5) we find

$$H_{\text{int}} = \frac{i}{\hbar}\left[H_{\text{HF}} + V^{\text{so}}, \; \sum_{i=1}^{N} \vec{r}_i \right] \cdot \frac{\vec{A}}{c} \;. \tag{A6}$$

Matrix elements of Eq. (A6) between exact eigenstates of the Hamiltonian $H_{\text{HF}} + V^{\text{so}}$ thus have the length form of the electric-dipole interaction. We emphasize that this result is not dependent on using H_{HF} for the zero-order Hamiltonian; instead, we might have used the exact spin-independent Hamiltonian to obtain the same result.

In fact, in this paper we did not solve $H_{\text{HF}} + V^{\text{so}}$ exactly, but rather solved the following model Hamiltonian exactly:

$$H_{\text{mod}} = H_{\text{HF}} + P_f V^{\text{so}} P_f \;. \tag{A7}$$

In Eq. (A7), P_f is a projection operator for the set of all final states having only one electron excited. In coordinate-space representation $P_f V^{\text{so}} P_f$ has the form:

$$\langle \vec{r}_1, \ldots, \vec{r}_N | \, P_f V^{\text{so}} P_f \, | \vec{r}_1', \ldots, \vec{r}_N' \rangle$$

$$= \sum_{i, j \in P_f} \langle \vec{r}_1, \ldots, \vec{r}_N | i \rangle \langle i | V^{\text{so}} | j \rangle \langle j | \vec{r}_1', \ldots, \vec{r}_N' \rangle . \tag{A8}$$

Note that in Eq. (A8) $\langle \vec{r}_i, \ldots, \vec{r}_N | i \rangle$ is the N-electron wave function for state i and $\langle i | V^{\text{so}} | j \rangle$ is a *number* and not an operator. Since the set P_f is incomplete, Eq. (A8) shows that $P_f V^{\text{so}} P_f$ is a nonlocal operator. As shown in Ref. 34, since we solve Eq. (A7) exactly in this paper, the coupling of electrons to the electromagnetic field is described by the length form of the electric-dipole operator.

In summary, then, we have shown that if a Hamiltonian containing V^{so} is solved exactly, then the momentum-dependence of V^{so} leads to the length form of the electric-dipole wave function. On the other hand, if only a part of V^{so} is included in one's model Hamiltonian (such as by restricting V^{so} to act within a particular subspace) one is led to a nonlocal potential, which according to Ref. 34 again leads to the length form for the electric-dipole interaction.

*Present address: Dept. of Physics, University of Notre Dame, Notre Dame, Ind. 46556.

[1]E. Fermi, Z. Phys. **59**, 680 (1930).

[2]F. L. Mohler and C. J. Boeckner, J. Res. Natl. Bur. Stand. **3**, 303 (1929).

[3]H. J. J. Braddick and R. W. Ditchburn, Proc. R. Soc. London Ser. A **143**, 472 (1934).

[4]M. J. Seaton, Proc. R. Soc. London Ser. A **208**, 418

(1951).

[5]U. Fano, Phys. Rev. 178, 131 (1969); 184, 250 (1969).

[6]J. Kessler and J. Lorenz, Phys. Rev. Lett. 24, 87 (1970).

[7]G. Baum, M. S. Lubell, and W. Raith, Phys. Rev. Lett. 25, 267 (1970).

[8]U. Heinzmann, J. Kessler, and J. Lorenz, Z. Phys. 240, 42 (1970).

[9]G. Baum, M. S. Lubell, and W. Raith, Phys. Rev. A 5, 1073 (1972).

[10]V. L. Jacobs, J. Phys. B 5, 2257 (1972).

[11]T. E. H. Walker and J. T. Waber, Phys. Rev. Lett. 30, 307 (1973); J. Phys. B 6, 1165 (1973).

[12]G. V. Marr, J. Phys. B 7, L47 (1974).

[13]E. J. McGuire, Phys. Rev. 161, 51 (1967).

[14]I. L. Beigman, L. A. Vainshtein, and V. P. Shevelko, Opt. Spectrosc. 28, 229 (1970).

[15]J. C. Weisheit, Phys. Rev. A 5, 1621 (1972).

[16]D. W. Norcross, Phys. Rev. A 7, 606 (1973).

[17]G. McGinn, J. Chem. Phys. 58, 772 (1973).

[18]J. J. Chang and H. P. Kelly, Phys. Rev. A 5, 1713 (1972).

[19]M. Ya. Amusia and N. A. Cherepkov, Case Stud. At. Phys. 5, 47 (1975), Fig. 26d.

[20]W. Ong and S. T. Manson, Phys. Lett. A 66, 17 (1978).

[21]H. A. Bethe and E. E. Salpeter, *Quantum Mechanics of One- and Two-Electron Atoms* (Springer-Verlag, Berlin, 1957), Chaps. 38 and 39.

[22]K. -N. Huang and A. F. Starace, Phys. Rev. A 18, 354

(1978).

[23]U. Fano and J. W. Cooper, Rev. Mod. Phys. 40, 441 (1968), Sec. 6.

[24]A. F. Starace, Phys. Rev. A 2, 118 (1970).

[25]W. Lotz, J. Opt. Soc. Am. 60, 206 (1970).

[26]G. Breit, Phys. Rev. 34, 553 (1929).

[27]K. -N. Huang, Phys. Rev. A 18, 1119 (1978).

[28]K. -N. Huang, Rev. Mod. Phys. (to be published).

[29]M. Blume and R. E. Watson, Proc. R. Soc. London Ser. A 270, 127 (1962).

[30]H. P. Kelly, Phys. Rev. B 136, 896 (1964); 144, 39 (1966).

[31]Our single-electron radial continuum HF wave functions for $l=1$ have the asymptotic form

$$R_{\epsilon l}(r) \xrightarrow[r \to \infty]{} (1/r)(2/\pi k)^{1/2} \sin[kr - \tfrac{1}{2}\pi + k^{-1}\ln 2kr$$

$$+ \arg \Gamma(l+1 - i/k) + \delta],$$

where $k \equiv [2\epsilon \,(\text{a.u.})]^{1/2}$.

[32]G. Breit and H. A. Bethe, Phys. Rev. 93, 888 (1954).

[33]S. Altshuler, Nuovo Cimento 3, 246 (1956).

[34]A. F. Starace, Phys. Rev. A 3, 1242 (1971); 8, 1141 (1973).

[35]T. B. Cook, F. B. Dunning, G. W. Foltz, and R. F. Stebbings, Phys. Rev. A 15, 1526 (1977).

[36]G. V. Marr and D. M. Creek, Proc. R. Soc. London Ser. A 304, 233 (1968).

[37]K. -N. Huang and A. F. Starace (unpublished).